Excitation and diagnosis of cascading Langmuir waves in ionospheric plasmas at Gakona, Alaska

2008 Phys. Scr. 2008 014030

(http://iopscience.iop.org/1402-4896/2008/T132/014030)

IOP Publishing Physica Scripta
Phys. Scr. **T132** (2008) 014030 (5pp) doi:10.1088/0031-8949/2008/T132/014030

Excitation and diagnosis of cascading Langmuir waves in ionospheric plasmas at Gakona, Alaska

L M Burton[1], J A Cohen[1], R Pradipta[1], A Labno[1], M C Lee[1,2], O Batishchev[1], D L Rokusek[1], S P Kuo[3], B J Watkins[4] and S Oyama[4]

[1] Massachusetts Institute of Technology, Cambridge, MA 02139, USA
[2] Boston University, Boston, MA 02215, USA
[3] Polytechnic University, Brooklyn, NY 11201, USA
[4] University of Alaska Fairbanks, Fairbanks, AK 99775, USA

E-mail: mclee@mit.edu

Received 2 April 2008
Accepted for publication 30 May 2008
Published 17 December 2008
Online at stacks.iop.org/PhysScr/T132/014030

Abstract
Ionospheric plasma heating experiments were conducted at Gakona, Alaska to investigate cascading spectra of Langmuir wave turbulence, excited by parametric instabilities diagnosed by Modular UHF Ionospheric Radar (MUIR). This work is aimed at testing the recent theory of Kuo and Lee (2005 *J. Geophys. Res.* **110** A01309) that addresses how the cascade of Langmuir waves can distribute spatially via the resonant and non-resonant decay processes. The non-resonant cascade proceeds at the location where parametric decay instability (PDI) or oscillating two-stream instability (OTSI) is excited and severely hampered by the frequency mismatch effect. By contrast, the resonant cascade, which takes place at lower matching heights, has to overcome the propagation loss of the Langmuir pump waves in each cascade step. Our experimental results have corroborated these predictions about the generation of cascading Langmuir waves by the HAARP heater.

PACS number: 94.20.wf

(Some figures in this article are in colour only in the electronic version.)

1. Introduction

The ionosphere can be used as a large plasma laboratory for controlled study of plasma turbulence. Research on the parametric excitation of Langmuir waves in ionospheric plasmas by ground-based HF heater has been actively conducted since the early 1970s (see e.g. reviews by Fejer 1979, Kuo 2001, 2004, Stenflo 2004, Stubbe 1996). This work deals with electromagnetic wave-induced Langmuir wave turbulence during plasma heating in space. This process can also occur in laser–plasma interactions. Cascade spectra of Langmuir waves were detected in ionospheric heating experiments by ground-based radars (see e.g. Carlson and Duncan 1977, Carlson *et al* 1972, Hagfors *et al* 1983, Lee *et al* 1997, 1998, 1999, Rietveld *et al* 2000, Stubbe *et al* 1992, 1994, Westman *et al* 1995) and by measurements of stimulated electromagnetic emissions (SEEs) (see e.g. Stubbe *et al* 1984, 1994, Thide *et al* 1982). The processes in the cascade of Langmuir waves manifested by the discrete feature of radar-detected HF enhanced plasma lines (HFPLs) are essential to the heating. The recent work of Kuo and Lee (2005) presents a theory to describe how Langmuir waves excited by O-mode heater waves via parametric decay instability (PDI) or oscillating two-stream instability (OTSI) can distribute spatially in ionospheric plasmas.

In brief, the theory developed by Kuo and Lee (2005) predicts two possible processes generating spectra of Langmuir waves via resonant and non-resonant cascading mechanisms. The non-resonant mechanism occurs at the same height where the PDI or OTSI is excited, to generate cascading Langmuir waves under the eigen-frequency mismatch condition. In the resonant process, the PDI- or OTSI-excited Langmuir wave will propagate to a lower altitude as a pump wave to excite Langmuir cascades via a parametric instability. The tradeoff is that the Langmuir pump wave experiences propagation attenuation before cascading occurs.

The instability thresholds under the frequency mismatch in the former process are found to be significantly greater than those under the propagation loss in the latter. Because of the lower instability thresholds, Kuo and Lee's theory predicts the following for experiments to verify. The resonant cascade process would be the dominating mechanism, which produces cascading spectra of Langmuir waves in several patches at different altitudes during the O-mode overdense heating of ionospheric plasmas.

We have conducted ionospheric heating experiments at Gakona, Alaska using the High-Frequency Active Auroral Research Program (HAARP) facility and Modular UHF Ionospheric Radar (MUIR) to investigate parametrically excited Langmuir waves discussed in Kuo and Lee (2005). In this paper, we present experimental results to provide evidence in support of the resonant cascade process in creating patches of cascading Langmuir waves at different altitudes. Our presentation is organized as follows. The theory of resonant and non-resonant cascade processes is briefly described in section 2. The experimental results and comparison with theoretical predictions are presented in section 3. In section 4, a summary is given and conclusions are finally drawn.

2. PDI-excited cascading Langmuir waves

The vertically transmitted O-mode heater wave can excite a Langmuir wave and an ion acoustic near but below its reflection height via the PDI or OTSI. The excited Langmuir wave (having wave frequency and wave vector denoted by (ω_1, $\mathbf{k}_1$)) can become a pump wave to parametrically excite a Langmuir sideband (ω_2, $\mathbf{k}_2$) and an ion-acoustic mode (ω_{s1}, $\mathbf{k}_{s2}$) as one cascade, where $\mathbf{k}_2 \approx -\mathbf{k}_1$ and $\mathbf{k}_{s2} \approx 2\mathbf{k}_1$. The cascade process obeys the wave frequency and wave vector matching relations, $\omega_1 = \omega_2 + \omega_{s2}*$ and $\mathbf{k}_1 = \mathbf{k}_2 + \mathbf{k}_{s2}$.

Using the coupled mode equations, derived from the electron and ion momentum and continuity equations, one can derive the dispersion relation for the cascading of PDI or OTSI as (Kuo and Lee 2005)

$$[\omega_2(\omega_2 + i\nu_e) - \omega_{k\theta}^2][\omega_{s2}^*(\omega_{s2}^* - i\nu_i) - 4k_1^2 C_s^2] \\ = k_1^2[k_0^2 + k_\perp^2\omega_1^2/(\omega_1^2 - \Omega_{ce}^2)](\omega_{pe}^4/\pi n_0 M \omega_{k\theta}^2)|\Phi_1|^2, \quad (1)$$

where Φ_1 is the Langmuir wave electric potential, ω_{pe} and Ω_{ce} the electron plasma and cyclotron frequencies, ν_e and ν_i the electron and ion damping rates, C_s the ion acoustic wave frequency, n_0 the background plasma density, M the ion mass, $\omega_{k\theta}^2 = \omega_{pe}^2 + 3k_{1z}^2 v_{te}^2 + \Omega_{ce}^2 \sin^2\theta_0$, where θ_0 is the angle between the local Earth's magnetic field and the Langmuir pump wave vector $\mathbf{k}_1$, and $k_\perp$ (k_0) is the perpendicular (parallel) component of $\mathbf{k}_1$ with respect to the Earth's magnetic field. The electron and ion damping rates include both particle elastic collisions and Landau damping rates ($\nu_e/2$ and $\nu_i/2$, respectively):

$$\nu_e/2 = (\pi/8)^{1/2}(\omega_0^2\omega_p^2/k_z k^2 v_{te}^3)\exp(-\omega_0^2/2k_z^2 v_{te}^2)$$

and

$$\nu_i/2 \approx (\pi/8)^{1/2}(\omega_s^2/k_s v_s) \\ \times \left[(m/M)^{1/2} + (T_e/T_i)^{3/2}\exp(-\omega_s^2/2k_z^2 v_{ti}^2)\right],$$

where k_z represents the component of $\mathbf{k}$ along the Earth's magnetic field.

As aforementioned, the O-mode wave-excited Langmuir wave can cascade into spectra of Langmuir waves with lower frequencies via resonant and non-resonant parametric instabilities until the instabilities saturate. These two possible mechanisms are examined below separately.

2.1. The resonant cascade process

In the process of resonant cascade, the Langmuir wave propagates downwards to excite a parametric instability at a lower altitude where the Langmuir sideband wave frequency satisfies the local dispersion relation, $\omega_2 = \omega_{k\theta}$, so $\omega_{s2} = 2k_1 C_s + i\gamma$ and $\omega_1 = \omega_{k\theta} + i\gamma$.

Substituting these relations into the dispersion relation (equation (1)), we get the threshold electric field amplitude of the instability as

$$|E_{th}| = \sqrt{\frac{meM}{e^2}}\sqrt{\frac{k_1 C_s \omega_{k\theta}^3 \nu_e \nu_i}{2\omega_{pe}^2[k_{1\parallel}^2 + (k_{1\perp}^2\omega_{k\theta}^2/\omega_{k\theta}^2 - \Omega_{ce}^2)]}}. \quad (2)$$

Since the pump wave propagates downwards, we have to consider spatial damping effects when calculating the field amplitude of the pump wave. Assuming a constant plasma density gradient, we can derive the distance propagated by the pump wave in between cascades to be:

$$\Delta z = \frac{4k_1 C_s \omega_1 L}{\omega_{pe}^2}, \quad (3)$$

where L is the scale length of the background plasma inhomogeneity. With the spatial damping rate from the imaginary component of the dispersion relation, we obtain the damping-rate factor of the pump wave field for each cascade:

$$f = \exp\left(\frac{2C_s \nu_e \omega_1^2 L}{3\omega_{pe}^2 v_{te}^2}\right), \quad (4)$$

where v_{te} is the electron thermal velocity.

2.2. The non-resonant cascade process

In the process of non-resonant cascade, the instabilities are excited at the same altitude as that of PDI or OTSI. The Langmuir pump wave frequency (ω_1) satisfies the local dispersion relation, $\omega_1 = \omega_{k\theta}$, so $\omega_{s2} = \omega_{s2r} + i\gamma$ and $\omega_2 = \omega_{k\theta} - \omega_{s2r} + i\gamma$.

With each cascade, the Langmuir sideband frequency decreases by twice the ion-acoustic frequency. Therefore, for N cascades, the sideband frequency is $\omega_{sNr} = \omega_{k\theta} - 2Nk_1 C_s$. Plugging this into the dispersion relation (equation (1)), we can solve for electric field threshold for N cascades as:

$$|E_{N\,th}| = \left(\sqrt{\frac{\nu_e}{\nu_e + 2N\nu_i}}\left[1 + \frac{16N^2k_1^2C_s^2}{\nu_e(\nu_e + 2N\nu_i)}\right]\right)^{1/2} \\ \times \sqrt{\frac{m_e M}{e^2}}\sqrt{\frac{k_1 C_s \omega_{k\theta}^3 \nu_e \nu_i}{2\omega_{pe}^2[k_{1\parallel}^2 + (k_{1\perp}^2\omega_{k\theta}^2/\omega_{k\theta}^2 - \Omega_{ce}^2)]}} \\ = \sqrt{G_N}|E_{th}|, \quad (5)$$

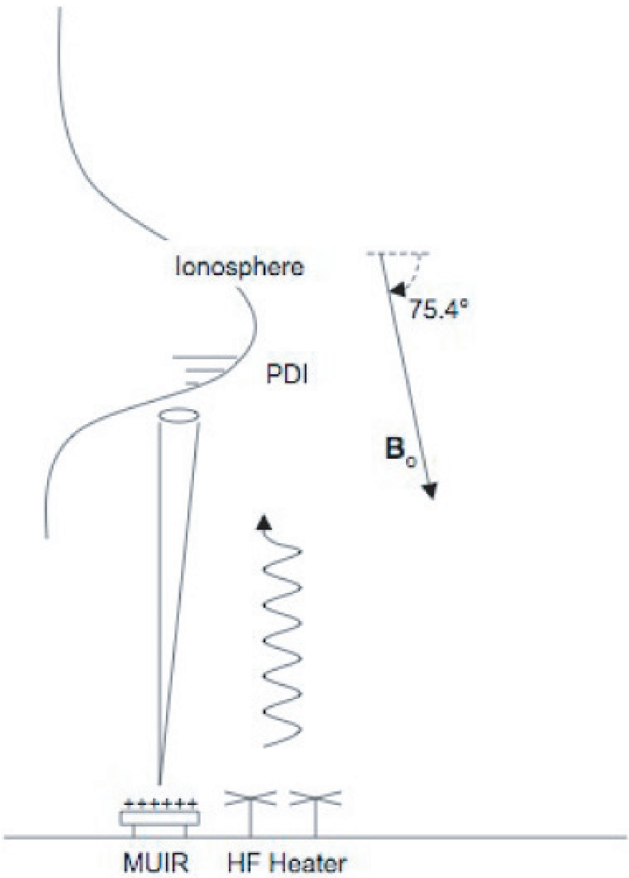

Figure 1. Experimental setup at HAARP. The HF heater and MUIR are co-located and the magnetic dip angle is 75.4°.

where G_N is the mismatch factor and $|E_{\rm th}|$ is the resonant decay threshold field (equation (2)). Generally, the mismatch factor is about 100 in the ionospheric *F* region, making the required threshold for the non-resonant decay 10 times larger than that for the resonant decay.

3. Gakona experiments

The data used to corroborate Kuo and Lee's theory was acquired from two separate Gakona experimental campaigns, the first in March 2006 and the second in August 2007. The experimental geometry is delineated in figure 1. The primary instruments used were the HAARP HF heater and the MUIR operating at 446 MHz. The characteristic features of MUIR can be found in Oyama *et al* (2006). For the March 2006 experiments, the heater's effective radiated power (ERP) was 80 MW at 4.3 MHz, yielding an estimated 1.2 V m^{-1} electric field at 230 km. As we conducted August 2007 experiments, the heater had been upgraded to an ERP of 398 MW at 3.3 MHz for an electric field of approximately 2.5 V m^{-1}. These calculations include the estimated swelling effect. We were able to detect the Langmuir waves produced by the HAARP heater via the Bragg scattering using the MUIR 446 MHz UHF diagnostic radar.

For the data analyses given below, we assumed that $T_{\rm e} = 1200$ K, $T_{\rm i} = 1000$ K, $\Omega_{\rm ce} = 2\pi \times 1.36$ MHz and $\nu_{\rm in} = 0.5\ {\rm s}^{-1}$ for the electron and ion temperature, electron cyclotron frequency and ion-neutral collision frequency, respectively.

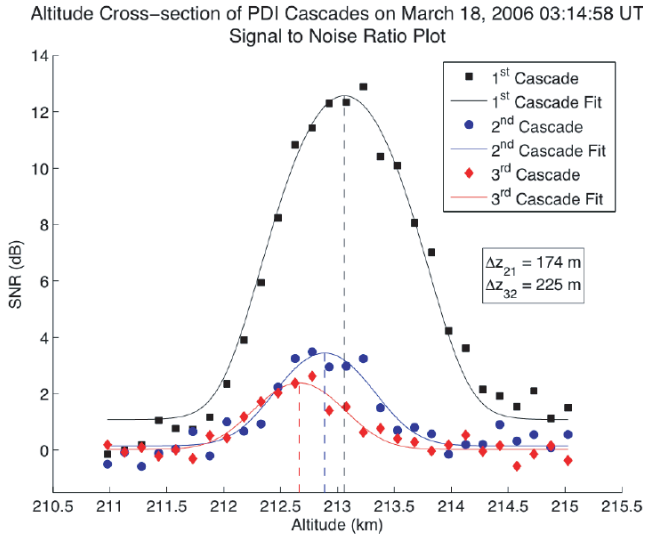

Figure 2. Altitude cross sections of MUIR data from 18 March, 2006 at 3 : 14 : 58 UT. The first cascade is marked with black squares, the second with blue circles and the third with red diamonds. A Gaussian curve fit is used to determine the peaks of the distribution. The altitude difference between the first and second cascades and between the second and third cascades is displayed below the legend.

The electron–ion collision frequency is dependent on the heater frequency, so for the 2006 experiments, $\nu_{\rm ei} = 470.7\ {\rm s}^{-1}$ for a heater frequency of 4.3 MHz, and for the 2007 experiments, $\nu_{\rm ei} = 277.2\ {\rm s}^{-1}$ for a heater frequency of 3.3 MHz. From those parameters, we derived $\upsilon_{\rm te} = 1.35 \times 10^5\ {\rm m\,s}^{-1}$, $\upsilon_{\rm ti} = 7.18 \times 10^2\ {\rm m\,s}^{-1}$ and $C_{\rm s} = 1.5 \times 10^3\ {\rm m\,s}^{-1}$ as the electron and ion thermal velocity and the acoustic speed in plasma. Using Bragg scattering, we calculated the wavenumber of the detected Langmuir wave as $k_0 = 6\pi\ {\rm m}^{-1}$. The electron plasma frequency was assumed to be approximately equal to the heater frequency, because PDI initiates at the reflection height of vertically transmitted heater wave.

3.1. Results from the March 2006 campaign

The March 2006 experimental campaign consisted of 4 days of 1–2 h long experiments on March 18, 23, 28 and 31. The best data occurred during the March 18 experiments at 3 : 14 : 58 UT. During this experiment, we transmitted an O-mode heater wave along the magnetic zenith (14° off the zenith, 202° azimuth) at 4.3 MHz CW, when the local peak plasma frequency was 4.5 MHz as determined by the HAARP digisonde on site. The MUIR antenna was directed along the magnetic zenith, transmitting coded-long pulses of 998 μs length with 10 ms IPP and 1 μs baud length, thus yielding 150 m range resolution.

MUIR detected three cascade lines, analyzed and displayed in figure 2. After isolating the altitude distribution of each line, the data showed a decreased SNR (signal-to-noise ratio) with altitude between each cascade. The figure shows the altitude cross-section of each cascade. The change in altitude between each cascade is measured from the peak. The intensity is in SNR (dB) relative to the average noise level. The changes in altitude were measured

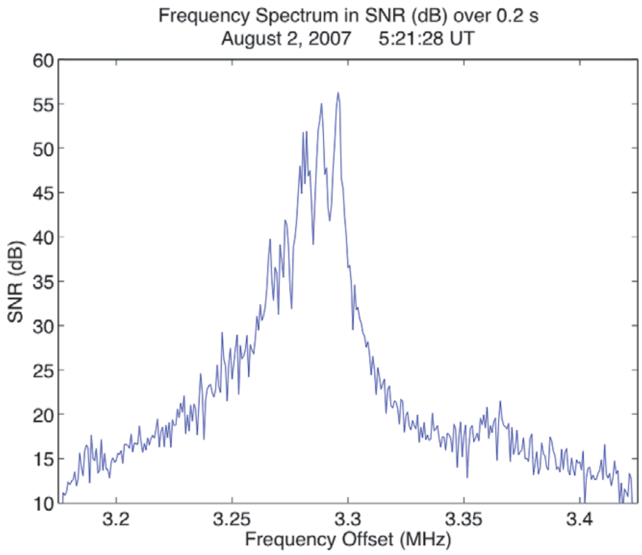

Figure 3. Frequency cross-section of MUIR data recorded on 2 August, 2007 at 5 : 21 : 29 UT. The intensity scaling is in dB relative to the average noise level integrated for 0.2 seconds.

as 174 m from the first to the second peak and 225 m from the second to the third peak, corresponding to ionospheric plasma inhomogeneity scale lengths of 41.9 and 54.2 km, respectively, using equation (3).

These observations were crosschecked with the predictions from the resonant and non-resonant decay theory. As mentioned earlier, the electric field amplitude of the injected wave is $\sim 1.2\,\mathrm{V\,m^{-1}}$. Using equation (4), the calculated wave field damping factor for scale lengths 41.9 and 54.2 km are 2.95 and 4.05, respectively. Using these wave field damping factors, the pump wave amplitude falls below the threshold of $0.075\,\mathrm{V\,m^{-1}}$ after undertaking three cascades. This agrees well with our observations with MUIR. When checked with the non-resonant cascade thresholds, only two cascades are expected, proving that the non-resonant cascade is not possible in this experiment. In addition, the frequency difference between two adjacent plasma lines ranges from 7.7 to 8.8 kHz, which is about twice the local ion acoustic wave frequency, reflecting the spectral characteristics of resonant cascade Langmuir waves.

3.2. Results from the August 2007 campaign

The August 2007 experimental campaign consisted of 4 days of 2–6 h long experiments from July 29 to August 2. The best data were taken on August 2 at 5 : 21 : 29 UT. During this experiment, we transmitted an O-mode heater wave at 3.3 MHz in pulsed mode (0.1 s ON, 4.9 s OFF) at the magnetic zenith. MUIR was oriented along the magnetic field, operating with an uncoded long pulse of 1 ms pulse length. On this occasion the MUIR was not operated with sufficient bandwidth to resolve the altitudes of individual cascade lines; we therefore focused on the number of cascades detected for comparison with the presented theory. Figure 3 shows a frequency cross section of the cascade lines. About six cascade lines were observed. The intensity is in SNR (dB) relative to the average noise level.

Using equation (5) for the non-resonant decay, the calculated threshold for six cascade lines is $1.19\,\mathrm{V\,m^{-1}}$. Thus, this does not rule out the non-resonant decay to occur with the heater field intensity increased to $2.5\,\mathrm{V\,m^{-1}}$. However, the frequency difference ($\sim$8 kHz) between two adjacent plasma lines is about twice the local ion acoustic wave frequency, showing the spectral characteristics of resonant cascade Langmuir waves. Furthermore, we can crosscheck the experimental results (i.e. the generation of six cascades) with the predictions for the resonant decay process as follows. According to equation (2) the threshold for resonant decay is $0.051\,\mathrm{V\,m^{-1}}$ with a heater frequency of 3.3 MHz. The predicted scale lengths range from 45 to 50 km (based on equation (3)), which corresponds to a field damping factor between 1.98 and 2.14 (based on equation (4)). These results are consistent with the observations made in March 2006 experiments.

4. Summary and conclusions

In this paper, we have shown that the data recorded from two Gakona campaigns at HAARP support the resonant cascade process as the primary cascade mechanism for O-mode heater wave-excited Langmuir waves. In the March 2006 experiments, we observed the decrease in altitude between cascades that is predicted in the resonant cascade process. The frequency spectra and the number of cascades, as well as the distance between cascades, are in excellent agreement with the theoretical model. Unfortunately, in the August 2007 campaign, we were unable to observe the decrease in altitude between cascades due to the MUIR instrument not being in a high-resolution mode. Nevertheless, we are able to compare the number of cascades for the two cascade models. While we could not disprove the non-resonant cascade mechanism, we found that the frequency spectra and the observed number of cascades yielded consistent predictions from the resonant cascade model as compared with those derived from the previous March 2006 experiments. Our work has demonstrated that the ionosphere provides an ideal plasma laboratory to investigate the spatial distribution of Langmuir wave turbulence excited by O-mode heater waves via PDI or OTSI.

Acknowledgment

This work was supported by the HAARP under ONR grants N00014-07-1-0999 and ONR-N00014-05-1-0109.

References

Carlson H C and Duncan L M 1977 HF excited instabilities in space plasmas *Radio Sci.* **12** 1001
Carlson H C, Gordon W E and Showen R L 1972 High-frequency induced enhancements of the incoherent scatter spectrum at Arecibo *J. Geophys. Res.* **77** 1242
Fejer J A 1979 Ionospheric modification and parametric instabilities *Rev. Geophys.* **17** 135
Hagfors T, Kofman W, Kopka H, Stubbe P and Aijanen T 1983 Observations of enhanced plasma lines by EISCAT during heating experiments *Radio Sci.* **18** 861
Kuo S P 2001 Cascade of the parametric decay instability in ionospheric heating experiments *J. Geophys. Res.* **106** 5593
Kuo S P 2004 On the cascade spectrum of Langmuir waves observed in Arecibo heating experiments *Phys. Scr.* **69** 115

Kuo S P and Lee M C 2005 Cascade spectrum of HF enhanced plasma lines generated in HF heating experiments *J. Geophys. Res.* **110** A01309 doi:10.1029/2004JA010674

Lee M C, Riddolls R J, Vilece K D, Dalrymple N E, Rowlands M J, Moriarty D T, Groves K M, Sulzer M P and Kuo S P 1997 Laboratory reproduction of Arecibo experimental results: HF wave-enhanced Langmuir waves *Geophys. Res. Lett.* **24** 115

Lee M C, Riddolls R J, Burke W J, Sulzer M P, Kuo S P and Klien E M C 1998 Generation of large sheet-like ionospheric plasma irregularities at Arecibo *Geophys. Res. Lett.* **25** 3067

Lee M C, Klien E M C, Burke W J, Zhang A X, Riddolls R J, Kuo S P, Sulzer M P and Isham B 1999 Augmentation of natural ionospheric plasma turbulence by HF heater waves *Geophys. Res. Lett.* **26** 37

Oyama S, Watkins B J, Djuth F T, Kosch M J, Bernhardt P A and Heinselman C J 2006 Persistent enhancement of the HF pump-induced plasma line measured with a UHF diagnostic radar at HAARP *J. Geophys. Res.* **111** A06309 doi:10.1029/2005JA011363

Rietveld M T, Isham B, Kohl H, LaHoz C and Hagfors T 2000 Measurements of HF-enhanced plasma and ion lines at EISCAT with high-altitude resolution *J. Geophys. Res.* **105** 7429

Stenflo L 2004 Comments on stimulated electromagnetic emissions in the ionospheric plasma *Phys. Scr.* T **107** 262

Stubbe P 1996 Review of ionospheric modification experiments at Tromso *J. Atmos. Terr. Phys.* **58** 34968

Stubbe P, Kopka H, Thide B and Derblom H 1984 Stimulated electromagnetic emission: a new technique to study the parametric decay instability in the ionosphere *J. Geophys. Res.* **89** 7523

Stubbe P, Kohl H and Rietveld M T 1992 Langmuir turbulence and ionospheric modification *J. Geophys. Res.* **97** 6285

Stubbe P, Stocker A J, Honary F, Robinson T R and Jones T B 1994 Stimulated electromagnetic emissions and anomalous HF wave absorption near electron gyroharmonics *J. Geophys. Res.* **99** 6233

Thide B, Kopka H and Stubbe P 1982 Observations of stimulated scattering of a strong high-frequency radio wave in the ionosphere *Phys. Rev. Lett.* **49** 1561

Westman A, Leyser T B, Wannberg G and Rietveld M T 1995 Tristatic EISCAT-UHF measurements of the HF modified ionosphere for low background electron temperature *J. Geophys. Res.* **100** 9717